Human Molecular Genetics, 2013, Vol. 22, No. 3 ***544–557***
doi:10.1093/hmg/dds465
Advance Access published on October 30, 2012

The molecular function and clinical phenotype of partial deletions of the *IGF2/H19* imprinting control region depends on the spatial arrangement of the remaining CTCF-binding sites

Jasmin Beygo[1,†], Valentina Citro[2,3,†], Angela Sparago[3,4], Agostina De Crescenzo[3], Flavia Cerrato[3], Melanie Heitmann[1], Katrin Rademacher[1], Andrea Guala[5], Thorsten Enklaar[6], Cecilia Anichini[7], Margherita Cirillo Silengo[8], Notker Graf[9], Dirk Prawitt[6], Maria Vittoria Cubellis[2], Bernhard Horsthemke[1], Karin Buiting[1,*] and Andrea Riccio[3,4,*]

[1]Institut für Humangenetik, Universitätsklinikum Essen, Essen, Germany, [2]Department of Structural and Functional Biology, University of Naples 'Federico II', 80126 Naples, Italy, [3]Department of Environmental Science, Second University of Naples, 81100 Caserta, Italy, [4]Institute of Genetics and Biophysics A. Buzzati-Traverso, CNR, 80131 Naples, Italy, [5]SOC Pediatria, Ospedale Castelli, Verbania (VCO), Italy, [6]Zentrum für Kinder- und Jugendmedizin, Universitätsmedizin Mainz, Mainz, Germany, [7]Dipartimento di Scienze Pediatriche e dell'Adolescenza, Università di Torino, Torino, Italy, [8]Department of Paediatrics, Obstetrics and Reproductive Medicine, University of Siena, Siena, Italy and [9]Zentrum für Humangenetik, Hildesheim, Germany

Received September 5, 2012; Revised and Accepted October 22, 2012

At chromosome 11p15.5, the imprinting centre 1 (IC1) controls the parent of origin-specific expression of the *IGF2* and *H19* genes. The 5 kb IC1 region contains multiple target sites (CTS) for the zinc-finger protein CTCF, whose binding on the maternal chromosome prevents the activation of *IGF2* and allows that of *H19* by common enhancers. CTCF binding helps maintaining the maternal IC1 methylation-free, whereas on the paternal chromosome gamete-inherited DNA methylation inhibits CTCF interaction and enhancer-blocking activity resulting in *IGF2* activation and *H19* silencing. Maternally inherited 1.4–2.2 kb deletions are associated with methylation of the residual CTSs and Beckwith–Wiedemann syndrome, although with different penetrance and expressivity. We explored the relationship between IC1 microdeletions and phenotype by analysing a number of previously described and novel mutant alleles. We used a highly quantitative assay based on next generation sequencing to measure DNA methylation in affected families and analysed enhancer-blocking activity and CTCF binding in cultured cells. We demonstrate that the microdeletions mostly affect IC1 function and CTCF binding by changing CTS spacing. Thus, the extent of IC1 inactivation and the clinical phenotype are influenced by the arrangement of the residual CTSs. A CTS spacing similar to the wild-type allele results in moderate IC1 inactivation and is associated with stochastic DNA methylation of the maternal IC1 and incomplete penetrance. Microdeletions with different CTS spacing display severe IC1 inactivation and are associated with IC1 hypermethylation and complete penetrance. Careful characterization of the IC1 microdeletions is therefore needed to predict recurrence risks and phenotypical outcomes.

*To whom correspondence should be addressed: Tel: +49 2017234555 (K.B.)/+39 0823274599 (A.R.); Fax: +49 2017235900 (K.B.)/+39 0823274605 (A.R.); Email: karin.buiting@uni-due.de (K.B.)/andrea.riccio@unina2.it (A.R.)
†These two authors are equally contributed.

INTRODUCTION

The Beckwith–Wiedemann syndrome (BWS, OMIM 130650) is a congenital disorder characterized by overgrowth, macroglossia, abdominal wall defects and predisposition to develop embryonal tumours, including Wilms' tumour and hepatoblastoma. The genetics of this pathology is complex, but the majority of the BWS cases is associated with abnormal expression of imprinted genes located in a large cluster at chromosome 11p15.5 (1). This cluster is organized in two regulatory domains, each including a specific imprinting control region (ICR, 2,3). The imprinted genes are expressed monoallelically and in a parent of origin-specific manner depending on the differential DNA methylation of the maternal and paternal alleles of the ICRs. Histone modifications likely contribute to the establishment and/or maintenance of the differential expression of the imprinted genes on the parental alleles (4,5).

The reciprocal imprinting of the fetal growth factor *IGF2* and the non-translated RNA *H19* genes is regulated by the telomeric ICR (IC1) of the 11p15.5 cluster. IC1 is a chromatin insulator that is located between *IGF2* and *H19*. Its function is mediated by interaction with the zinc-finger protein CTCF that by inducing allele-specific higher-order chromatin conformations prevents the activation of *IGF2* promoters by downstream enhancers on the maternal chromosome (6–8). On the paternal chromosome, germline-derived DNA methylation inhibits CTCF binding, resulting in inactivation of the insulator and expression of *IGF2* (3). In addition, due to CTCF binding, the maternal IC1 is maintained in a methylation-free status (9).

Heterogeneous molecular defects are present at 11p15.5 in the individuals affected by BWS (1). The most frequent ones are DNA methylation abnormalities affecting either one of the two ICRs or paternal uniparental disomy affecting the entire cluster. In particular, gain of DNA methylation at the maternal IC1 results in the loss of CTCF binding and changes in chromatin conformation favouring *IGF2* activation and *H19* silencing (6). Although in many cases aberrant IC1 methylation has not been associated with any evident sequence change, several microdeletions within IC1 were described in BWS and Wilms' tumour cases (10–18). However, the penetrance of the clinical phenotype associated with these genetic defects and the molecular mechanism by which they alter *IGF2-H19* imprinting are undefined.

Human IC1 is composed by repetitive modules containing six to seven CTCF target sequences (CTS, Fig. 1). When maternally transmitted, 1.4–1.8 kb deletions removing one to two CTSs were found associated with hypermethylation of the remaining CTSs, loss of *IGF2-H19* imprinting and highly penetrant BWS phenotype (10,11,13,17). In contrast, a 2.2 kb deletion removing three CTSs was not associated with DNA hypermethylation and was accompanied by a secondary mutation in one of the individuals affected by BWS (12,19). To explain these differences in the clinical phenotype, we proposed that different spatial arrangements of CTSs were associated with different IC1 activities (13). Consistent with this hypothesis, a microduplication associated with IC1 hypermethylation was later identified in a familial case with Wilms' tumour and BWS (18). However, more recently, factors other than CTCF, such as OCT4 and SOX2, have been implicated in IC1 imprinting control (15,20).

To prove that CTS arrangement within IC1 affects the mechanisms controlling genomic imprinting and ultimately influences the phenotype, we analysed several characteristics of the mutant IC1 alleles, both *in vivo* and *in vitro*. We demonstrated that DNA methylation in peripheral blood cells, and enhancer-blocking activity and binding to CTCF in cultured cells are influenced by the spatial organization of the CTSs, rather than their number. The results obtained are useful to predict the clinical phenotype resulting from IC1 mutations.

RESULTS

New clinical cases and summary of the IC1 microdeletions

Using MS-MLPA (methylation-specific multiplex ligation-dependent probe amplification), we identified a microdeletion in peripheral blood from a female patient (family 8 III.1) presenting with classical features of BWS, like hemihyperplasia, macroglossia, hypoglycaemia and ear creases. Methylation analysis by MLPA revealed a slight hypermethylation for all methylation sensitive probes in the IC1 outside the deletion (data not shown). The deletion was also found in the healthy mother and maternal aunt, who have inherited the deletion from their healthy father (maternal grandfather of the patient). All three unaffected deletion carriers showed normal methylation in the IC1 region. The deletion was confirmed by long-range PCR, and sequence analysis of the deletion breakpoints revealed that the deletion is 2.245 kb in size (GenBank Accession No. AF125183: 5710–5720/7955-7965). It abolishes the repeats B2, B3, B4 and A2 including the CTSs 4 and 5 and fuses CTS3 and 6 within the repeats B5 and B1 (Fig. 1). Interestingly, the microdeletion is identical on the nucleotide level to a familial case reported by Prawitt *et al*. (12) (family 7 in this paper), including single nucleotide variants which are in phase with the deletion allele (Table 1). In this family, one patient (III.1) was described to have a duplication of 11p15 in fibroblasts as detected by fluorescence *in situ* hybridization (FISH), which was not found in a healthy carrier (12). We did not find an 11p15 duplication in the blood of another patient (III.2) of family 7 who was investigated further in this study, nor in patient III.1 of family 8 by MLPA.

We also found a 0.8 kb deletion fusing the B3 with the B1 repeat and removing CTSs 4 and 5 (Fig. 1) in several individuals of a family, none of which was affected by BWS (family 9, Supplementary Material, Fig. S1). However, in all these individuals the 0.8 kb deletion was paternally inherited.

The 2.2 kb deletion (families 7 and 8) and 0.8 kb deletion (family 9) add to a number of previously described IC1 microdeletions, including the 1.4 kb (fusing B5 with B3, family 3), the 1.8 kb (fusing B6 with B3, families 2 and 4) and the 1.8 kb (fusing B5 with B2, family 6) (Fig. 1 and 10,11,13,17). Breakpoints and sequence variants of the IC1 alleles investigated are reported in Table 1. The clinical characteristics of the individuals under study are described in Table 2.

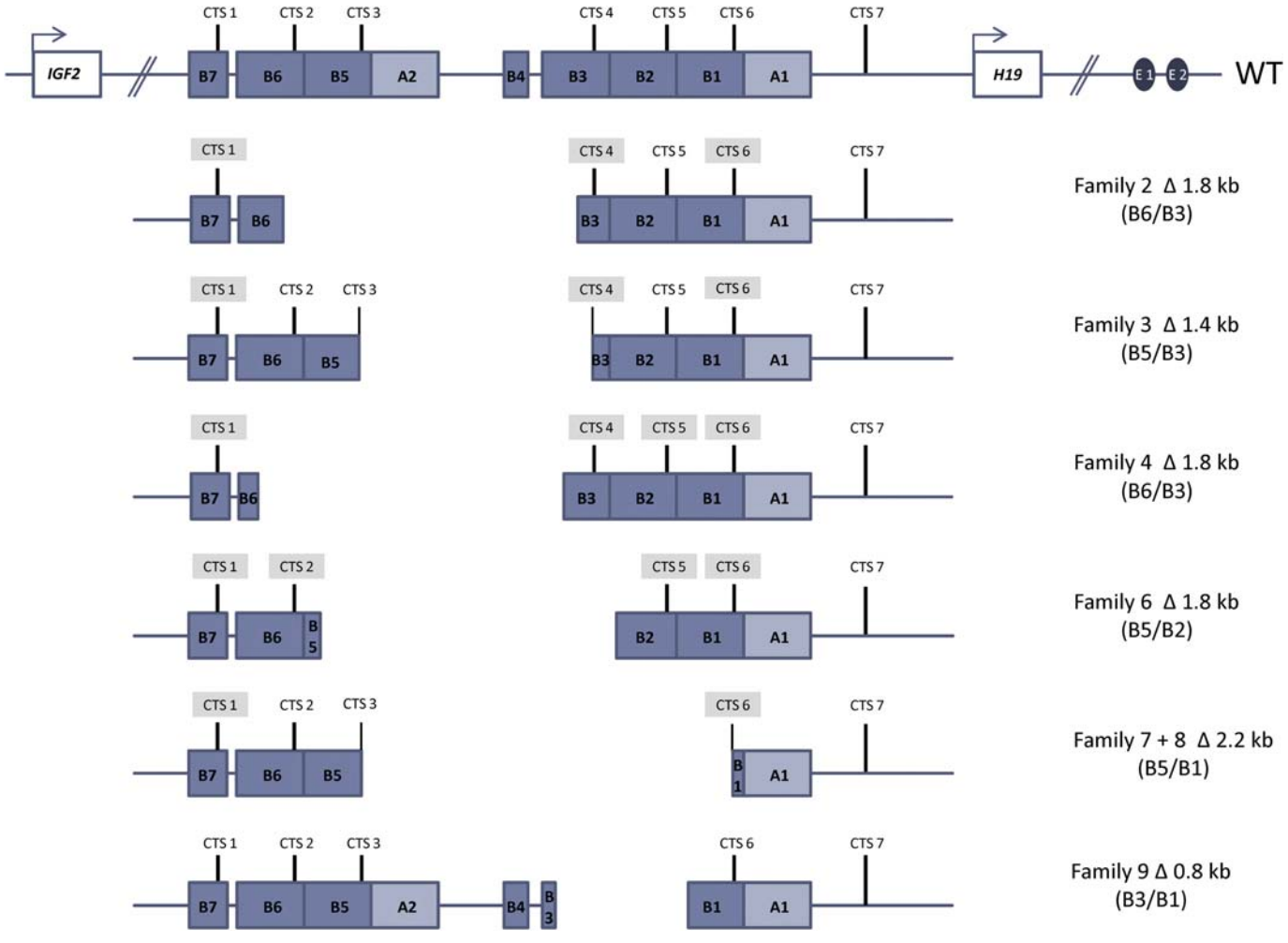

Figure 1. IC1 microdeletions investigated in this study. Blank spaces correspond to deleted sequences. The positions of the CTS1–7 and the organization in A-type and B-type repeats are shown for each IC1 allele. The relative positions of the *IGF2* and *H19* genes and the common enhancers are indicated only for the wild-type allele. The CTSs whose methylation is analysed by NGS are highlighted.

DNA methylation analysis of the IC1 DMR by next generation bisulfite sequencing

To obtain highly quantitative DNA methylation patterns at the IC1 DMR in individuals carrying different IC1 deletions, we performed high-resolution methylation analysis on peripheral blood leukocyte (PBL) DNAs using next generation bisulfite sequencing on the Roche/454 Genome Sequencing junior system. In normal controls, the IC1 DMR is methylated on the paternal and unmethylated on the maternal chromosome.

First we established different PCR assays specific for the six CTSs and for the respective deletions. We investigated the effect on DNA methylation in affected and non-affected deletion carriers from six families with different IC1 deletions. For each deletion carrier, we separately amplified the wild-type (WT) allele and a fusion product for the corresponding deletion allele containing one CTS. Furthermore, we investigated additional CTS without separating the alleles. We investigated CTS1 and CTS6 in all families (Fig. 2), CTS2 in family 6, CTS4 in families 2–4 and CTS5 in families 4 and 6 (Supplementary Material, Fig. S2). The number of CpG dinucleotides for each CTS studied is listed in Table 3. For each of the six CTSs, we analysed six normal individuals. An average of 47.9 to 54.9% mean methylation per CTS was observed (Supplementary Material, Table S1) and the average of the mean methylation over all CTSs was 52.9%.

In three families with different 1.8 kb deletions, we investigated the index patients and the mothers, who are also deletion carriers. As expected, the healthy mother (II-5) of family 2, who has inherited the deletion from her father, showed a normal methylation pattern for CTS1 and 6 (alleles were not separated) of 55.4 and 56.8%, respectively, whereas the son showed a hypermethylation of 93.8 and 86.5%, respectively (Fig. 2B and C; Table 3). Methylation analysis for CTS4, where the alleles were separated, provided nearly the same result. Here, too, the mother showed no methylation changes, but the affected son (III-3) showed a mean methylation of 95.4% at CTS4 on the maternal deletion allele (Supplementary Material, Fig. S2B).

In family 4, the 1.8 kb deletion is similar to that in family 2, but in this family both the mother (II-1) and the son (III-2) are affected and have the deletion on the maternal chromosome.

Table 1. Nucleotide variants in IC1 alleles

Allele	Breakpoint[a]	Variants[a] 4593	4628	4721	6368	7342	7357	7523	7966	8008	8097	8217	8271
Wild-type		A	T	G	C	G	G	G	T	A	G	G	T
Δ 0.8 B3/B1 (family 9)	6899-6941/ 7712-7754	G	C	A	C	—	—	—	T	A	G	G	T
Δ 1.8 B6/B3 (family 2)	5297-5314 /7131-7148	A	T	G	—	G	G	A	T	A	G	G	T
Δ 1.4 B5/B3 (family 3)	5723-5752/ 7156-7185	A	T	G	—	G	G	A	C	C	A	C	C
Δ 2.2 B5/B1 (families 7,8)	5710-5720 /7955-7965	A	T	G	—	—	—	—	T	A	G	G	T
Δ 1.8 B5/B2 (family 6)	5469-5516/ 7304-7350	A	T	G	—	A	A	G	T	A	G	G	T

[a]Breakpoint and variant positions within GenBank accession N° AF125183.

Interestingly, methylation analysis at CTS1 for the deletion alleles revealed different levels of mean methylation; the mother has 70.7% and the patient 93.4% (Fig. 2B and Table 3). This inter-individual difference in methylation at CTS1 in these two individuals confirms previous results obtained by combined bisulfite restriction analysis (COBRA, 11). Additionally, CTS4, 5 and 6 were investigated without allele separation. At these sites, both, the patient and the mother showed severe hypermethylation; however, again the level of methylation seems to be slightly lower in the mother than in the patient but not as pronounced as at CTS1 (Table 3, Fig. 2C and Supplementary Material, Fig. S2B and C).

In family 6, where the 1.8 kb deletion covers the more distal region of IC1, we analysed separate alleles for CTS2 and CTS5 in the affected mother and the index patient. Both carry the deletion on the maternal chromosome. On the deletion allele the mother showed 81.4% mean methylation at CTS2 and 80.4% at CTS5 (Supplementary Material, Fig. S2A and C and Table S3). The deletion allele of the patient showed a slightly higher methylation level of 89.5% at CTS2 and 94.5% at CTS5. Again, CTS1 and 6 were analysed without separating the alleles. Mother and patient showed high methylation levels of 89.6 and 95.7%, respectively, for CTS1. For CTS6 a similar tendency was observed, but the methylation levels were with 68.7 and 84.2% not as high as at the other investigated CTS (Fig. 2B and C).

In family 3, we found for the index patient (II-1), who has a *de novo* deletion of 1.4 kb, an extensive hypermethylation at CTS4 of 85.1% on the maternal deletion allele (Supplementary Material, Fig. S2B and Table S3). CTS1 showed for both alleles together a methylation level of 95.1%, whereas CTS6 was a bit lower with 82.7% (Fig. 2B and C).

In family 7 and 8 with the identical 2.2 kb deletion, the two individuals with BWS (III.2, family 7 and III.1, family 8), who have a maternally inherited IC1 deletion, were found to have a methylation of 17.0 and 33.9% at the maternal CTS6, respectively. As expected, the two healthy deletion carriers of family 8 (II.2 and II.3) with a paternally inherited deletion have a methylated deletion and an unmethylated WT allele (Fig. 2C and Table 3). But most interestingly, the mother (II.5) of family 7 and the grandfather (I.1) of family 8 show very little (4.0%) or no (0.8%) evidence of methylation changes on the deletion allele, although they have inherited the deletion from their mothers. Moreover, both individuals do not have BWS (12 and this study). These results are supported by methylation analyses of CTS1 without separating the alleles, where similar results were obtained in the two patients who show a slight hypermethylation of 68.0% (III.2 family 7) and 72.0% (III.1 family 8), whereas the mother and aunt (II.2 and II.3) of family 8 show normal methylation levels ∼50% (Fig. 2B and Table 3). The mother (II.5) of family 7 and the grandfather (I.1) of family 8, however, show a moderate hypermethylation at CTS1 of 71 and 64%, respectively, similar to the patients.

Enhancer blocking assay

To study the effect of the microdeletions on IC1 function, we amplified the mutant IC1 alleles from patient DNAs, cloned them into plasmid vectors and tested their functional properties by transferring them into cultured cells. First, we measured the insulator activity by using the previously described enhancer-blocking assay (21,22). For this purpose, we generated constructs (EpL) in which the WT or mutant IC1 sequences were inserted between the SV40 enhancer (E) and the SV40 promoter (p) that was driving the luciferase gene (L) (Supplementary Material, Fig. S3). In addition to the WT IC1, the tested alleles included the 0.8 kb (B3/B1, family 9), 2.2 kb (B5/B1, family 7/8), 1.4 kb (B5/B3, family 3), 1.8 kb (B6/B3, family 2) and 1.8 kb (B5/B2, family 6) deletions.

The constructs were introduced into Hep3B cells and pools of stably transfected clones were isolated. Copy number of exogenous DNAs was calculated and found to be similar among different transfected samples (data not shown). CpG methylation of the exogenous IC1 alleles was measured by COBRA and bisulfite sequencing and all integrated constructs were found non-methylated in Hep3B cells.

Reporter gene activity was then measured in the transfected cells. Consistent with the presence of the SV40 enhancer, the luciferase activity expressed by the EpL construct was 3.6-fold higher than that of the enhancer-less construct (pL; Fig. 3 and Supplementary Material, Table S3). A control construct (E spacer λ pL), in which a 5090 bp fragment of the λ phage was inserted between the promoter and the enhancer, showed luciferase activity similar to EpL, indicating that within these limits the distance does not affect the enhancer activity. The luciferase activity of the WT IC1 allele (E wt pL) was 27% that of the control (E spacer λ pL) and close to the activity expressed by the enhancer-less construct pL, confirming the presence of enhancer-blocking activity in the WT IC1 fragment. Different reporter activities were expressed by the mutant alleles (Fig. 3). In particular, the activities of the 0.8 kb (B3/B1) and 2.2 kb (B5/B1) deletion alleles were 39

Table 2. Clinical features of the individuals maternally inheriting the IC1 microdeletions

Families	2	3	4			6		7					8	
	Δ1.8 kb (B6/B3)	Δ1.4 kb (B5/B3)	Δ1.8 kb (B6/B3)			Δ1.8 kb (B5/B2)		Δ2.2 kb (B5/B1)					Δ2.2 kb (B5/B1)	
Individuals	III-3	II-1	II-1	III-2		II-2	III-1	II.5	III.1	III.2	III.4	III.5	III.6	I.1	III.1
Clinical features															
Birth weight > 90th centile	−	−	+	+		+	+	Unaffected carrier	+	+	Unaffected carrier	+	Unaffected carrier	Unaffected carrier	+
Postnatal overgrowth	+	−	−	−		−	−		+	+		+			+
Macroglossia	+	+	+	+		+	+		+	+		+			+
Abdominal wall defect	+	+	−	−		−	+		+	+		−			−
Pits and creases	−	−	−	+		−	+		−	+		+			+
Hypoglycaemia	+	−	−	+		−	+		−	−		−			+
Polyhydramnios	+	−	−	−		−	+		−	−		−			−
Neavus flammeus	+	+	−	−		−	−		−	−		−			−
Hemihypertrophy	+	−	−	+		−	−		+	−		−			+
Organomegaly	+	−	−	−		−	+		+	+		+			−
Childhood cancer	−	−	−	+		−	−		+	+		+			−
Urogenital abnormalities	−	+	−	−		+	+		−	−		−			−
Others	−	−	Congenital stiff neck	−		−	−		Hypertelorism	Hypertelorism	Unaffected carrier	Hypertelorism	Unaffected carrier	Unaffected carrier	−

and 31% that of the λ spacer, respectively, while those of the 1.4 kb (B5/B3), 1.8 kb (B6/B3) and 1.8 (B5/B2) deletion alleles were 70, 56 and 63% that of the control. Therefore, the Δ 1.4 kb (B5/B3), Δ 1.8 kb (B6/B3) and Δ 1.8 kb (B5/B2) alleles displayed lower insulator activity than the Δ 0.8 kb (B3/B1), Δ 2.2 kb (B5/B1) alleles and WT alleles.

To further investigate the role of the A2-B4 region that is missing in both high-insulating and low-insulating alleles, we generated *in vitro* two additional mutant constructs (Fig. 4). In the former (ΔA2), the entire A2-B4 modules but no CTS was deleted and in the latter (OCT-mut), three OCT-binding motifs present within the A2 region were mutated in the WT IC1 allele. After transfection in Hep3B cells, we found that the luciferase activity expressed by the A2 deletion (E Δ A2 pL) and OCT-mut (E OCT-mut pL) constructs was 70 and 40% that of the control construct, respectively (Fig. 4), indicating that the insulator activity of the WT allele is severely affected by the deletion of the A2-B4 spacer but modestly influenced by the mutation of the OCT-binding motifs.

Analysis of CTCF binding

Since CTCF binding is required for the enhancer-blocking function of IC1 (21,22), we wondered if the mutant alleles with different insulator activities also bound CTCF *in vivo* with different efficiencies. The presence of endogenous CTCF was previously demonstrated in Hep3B cells (21). Therefore, we measured CTCF binding to the different IC1 alleles by the Chromatin ImmunoPrecipitation (ChIP) assay with anti-CTCF antibodies in transfected Hep3B cells. We estimated the amount of IC1-containing DNA fragments present in the immunoprecipitated material by quantitative PCR. To specifically detect exogenous DNA, we used a set of PCR primers that was specific for the transfected constructs and was targeting sequences close to CTS1. Another set of primers, targeting CTS6, was not construct specific. The samples were normalized against an endogenous region that was demonstrated to bind CTCF with high affinity (23). Figure 5 and Supplementary Material, Table S3 show the results obtained for CTCF binding to the transfected constructs by using primers close to CTS1. The construct containing WT IC1 bound CTCF with the highest efficiency. The 0.8 kb (B3/B1) and the 2.2 kb (B5/B1) deletion alleles showed values of binding that were 1.2 and 1.4-fold lower than that of the WT construct, respectively. The 1.4 kb (B5/B3), 1.8 kb (B6/B3), 1.8 (B5/B2) and A2 deletion alleles showed weaker CTCF binding. The amount of exogenous IC1 DNA immunoprecipitated from the Δ 1.4 kb (B5/B3), Δ 1.8 kb (B6/B3), Δ 1.8 kb (B5/B2) and Δ A2 alleles was\xEF\x80 3.3-, 2.6-, 7.4- and 4.2-fold lower than that of the WT, respectively. In addition, the construct bearing the mutation of the OCT-binding sites showed CTCF binding values that were only 1.4-fold lower than that of the WT allele. Comparable results were obtained from the analysis of CTCF binding to CTS6 (Supplementary Material, Fig. S4 and Table S3).

DISCUSSION

Possibly, due to the presence of low-copy repeats, the IC1 of the *IGF2-H19* locus undergoes structural rearrangements resulting in cryptic microdeletions. These deletions are

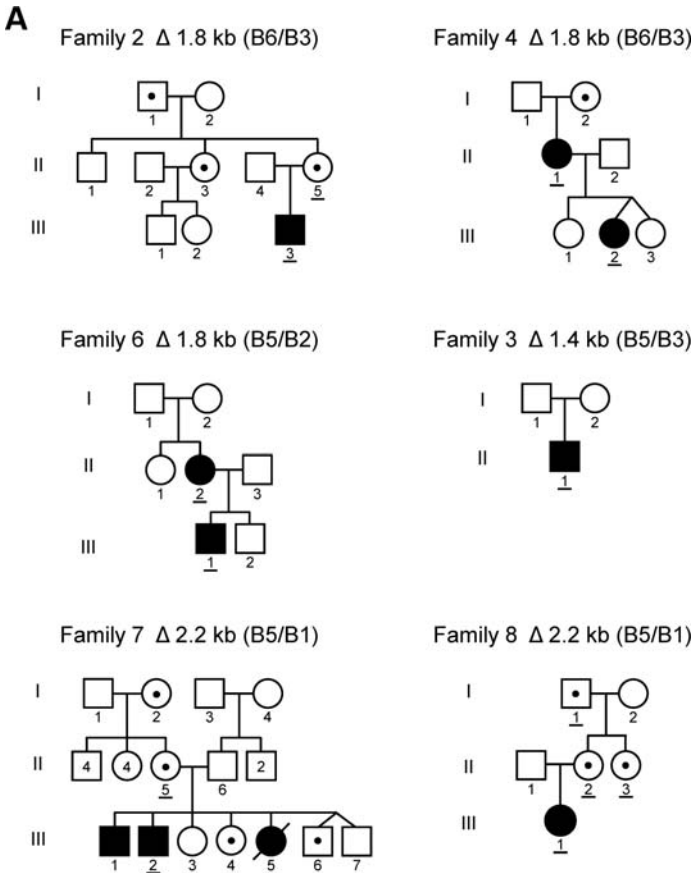

Figure 2. DNA methylation analysis. (**A**). Pedigrees of the families investigated. The individuals studied are underlined. Unaffected deletion carriers are indicated by a dot. (**B** and **C**). Heatmaps for the methylation patterns obtained by next generation bisulfite sequencing for CTS1 and 6, respectively. The methylation pattern of a normal control (NC) is shown on the left side. The methylation analyses were performed with or without allele separation for each deletion carrier investigated. The results were arranged according to their parental origin. In the heatmaps of individuals, III.2 of family 7 and III.1, II.2 and II.3 of family 8 a blue column inside methylated sequences represent a SNP (rs10732516 C>T) which changes a CpG to a TpG and therefore is scored as unmethylated by the BiQ Analyzer software. Lines represent sequence reads, columns CpGs. Blue—unmethylated; red—methylated; white—missing sequence information; mat, maternal allele; pat, paternal allele; del, allele harbouring the IC1 deletion; WT, wild-type allele; NC, normal control; CTS, CTCF target site.

associated with a spectrum of phenotypes spanning from normal condition to complete BWS with Wilms' tumour. By analysing the mutant alleles both *in vivo* and *in vitro*, we demonstrate that the microdeletions generally affect IC1 function and binding to CTCF. However, the extent of IC1 inactivation and consequently the penetrance and expressivity of the clinical phenotype are dependent on the structural arrangement of the residual CTSs of the microdeletion alleles.

CTCF binding is required to maintain the maternal IC1 hypomethylated during early embryogenesis (9). The analysis of several IC1 mutations in the mouse indicates that the lower the residual affinity for CTCF, the higher the gain of methylation on the maternal IC1 allele (24). Therefore, the maternal methylation level can be considered as an indirect measure of CTCF binding to the mutant allele in the embryo. By analysing patient PBLs, we found that when present on the maternal chromosome the human 2.2 kb (B5/B1) deletion results in variable but generally moderate methylation of the remaining CTS1 and 6 (4–34%), whereas the 1.4 kb (B5/B3) and 1.8 kb (both B5/B2 and B6/B3) deletions are generally associated with more consistent hypermethylation (69–96%). This is consistent with the results reported by Demars *et al*. Analysis of CTCF binding in cells transfected with the mutant alleles indicated that binding to IC1 is partially affected by the 2.2 kb (B5/B1) deletion but severely disrupted by the 1.4 kb and 1.8 kb deletions. Therefore, it is possible that during early embryogenesis low CTCF binding results in frequent *de novo* methylation of the 1.4 and 1.8 kb deletion alleles, whereas moderate binding results in stochastic methylation of the 2.2 kb deletion allele. It might also be possible that oocytes with the deletion alleles are erroneously methylated and some of this methylation is subsequently lost by failure to maintain the methylation. Both interpretations are consistent with the mosaic state of methylation which can be seen to a larger extent in the 2.2 kb deletion carriers but also through the slight inter-individual differences in the degree of methylation at different CTS in most individuals with a 1.4 or 1.8 kb deletion, as they still have a small amount of unmethylated sequences left.

We note with interest that the hypermethylation is more pronounced in the second generation of families with two affected generations so that it is tempting to speculate that

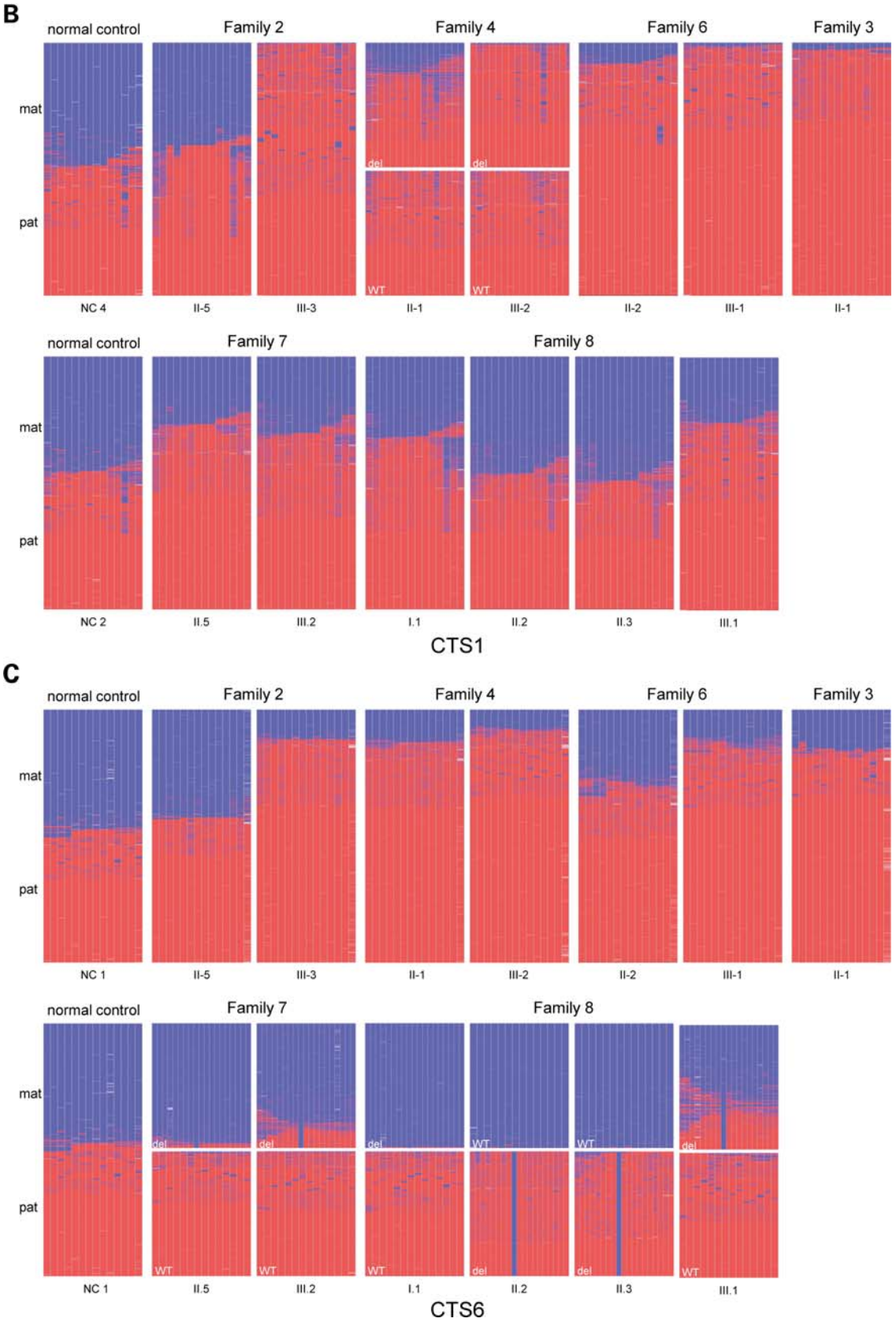

Figure 2. *Continued*

Table 3. Summary of the results obtained by next generation bisulfite sequencing for the six families investigated

	ID		Status	Allele harbouring the deletion	Mode of inheritance	CTS investigated	Number of investigated CpGs	Alleles	Sequence reads	Mean methylation (%)
Family 2 [a,d]Δ 1.8 kb (B6/B3)	II-5	Mother	Healthy carrier	Paternal	Paternally	CTS1	14	Both alleles	2222	55.4
	III-3	Patient	Affected	Maternal	Maternally		14	Both alleles	2417	93.8
	II-5	Mother	Healthy carrier	Paternal	Paternally	CTS4	16	Mat WT	1275	2.4
							21	Pat Del	5609	92.1
	III-3	Patient	Affected	Maternal	Maternally		21	Mat Del	1220	95.4
							16	Pat WT	1285	96.3
	II-5	Mother	Healthy carrier	Paternal	Paternally	CTS6	14	Both alleles	2068	56.8
	III-3	Patient	Affected	Maternal	Maternally		14	Both alleles	1784	86.5
Family 3 [c,d]Δ 1.4 kb (B5/B3)	II-1	Patient	Affected	Maternal	De novo	CTS1	14	Both alleles	2144	95.1
	II-1	Patient	Affected	Maternal	De novo	CTS4	21	Mat Del	3545	85.1
							16	Pat WT	2318	92.5
	II-1	Patient	Affected	Maternal	De novo	CTS6	14	Both alleles	3139	82.7
Family 4 [d] Δ 1.8 kb (B6/B3)	II-1	Mother	Affected	Maternal	Maternally	CTS1	16	Mat del	2214	70.7
							16	Pat WT	1655	93.7
	III-2	Patient	Affected	Maternal	Maternally		16	Mat del	3006	93.4
							16	Pat WT	1218	93.9
	II-1	Mother	Affected	Maternal	Maternally	CTS4	16	Both alleles	1444	85.6
	III-2	Patient	Affected	Maternal	Maternally		16	Both alleles	1454	96.5
	II-1	Mother	Affected	Maternal	Maternally	CTS5	14	Both alleles	2159	91.6
	III-2	Patient	Affected	Maternal	Maternally		14	Both alleles	2192	95.4
	II-1	Mother	Affected	Maternal	Maternally	CTS6	14	Both alleles	3235	84.7
	III-2	Patient	Affected	Maternal	Maternally		14	Both alleles	3170	89.7
Family 6 [e]Δ 1.8 kb (B5/B2)	II-2	Mother	Affected	Maternal	De novo	CTS1	14	Both alleles	1919	89.6
	III-1	Patient	Affected	Maternal	Maternally		14	Both alleles	1726	95.7
	II-2	Mother	Affected	Maternal	De novo	CTS2	19	Mat del	707	81.4
							20	Pat WT	537	94.9
	III-1	Patient	Affected	Maternal	Maternally		19	Mat del	926	89.1
							20	Pat WT	1107	95.8
	II-2	Mother	Affected	Maternal	De novo	CTS5	15	Mat del	3423	80.4
	III-1	Patient	Affected	Maternal	Maternally		15	Mat del	1576	94.5
	II-2	Mother	Affected	Maternal	De novo	CTS6	14	Both alleles	1916	68.7
	III-1	Patient	Affected	Maternal	Maternally		14	Both alleles	1816	84.2
Family 7 [b]Δ 2.2 kb (B5/B1)	II.5	Mother	Healthy	Maternal	Maternally	CTS1	14	Both alleles	3293	71.4
	III.2	Patient	Affected	Maternal	Maternally		14	Both alleles	2433	68.0
	II.5	Mother	Healthy	Maternal	Maternally	CTS6	19	Mat del	4922	4.0
							14	Pat WT	1697	95.3
	III.2	Patient	Affected	Maternal	Maternally		19	Mat del	1226	17.0
							14	Pat WT	3718	95.3

Continued

Table 3. *Continued*

	ID	Status	Allele harbouring the deletion	Mode of inheritance	CTS investigated	Number of investigated CpGs	Alleles	Sequence reads	Mean methylation (%)
Family 8 Δ 2.2 kb (B5/B1)	III.1	Patient	Affected	Maternal	Maternally	CTS1	14	Both alleles	2345	72.0
	II.2	Mother	Healthy carrier	Paternal	Paternally		14	Both alleles	3766	52.8
	II.3	Aunt	Healthy carrier	Paternal	Paternally		14	Both alleles	3747	50.5
	I.1	Grand father	Healthy carrier	Maternal	Unknown		14	Both alleles	2384	63.9
	III.1	Patient	Affected	Maternal	Maternally	CTS6	19	Mat del	1003	33.9
							15	Pat WT	2002	93.6
	II.2	Mother	Healthy carrier	Paternal	Paternally		14	Mat WT	2894	0.4
							19	Pat del	3044	88.7
	II.3	Aunt	Healthy carrier	Paternal	Paternally		14	Mat WT	1346	0.4
							19	Pat del	676	87.8
	I.1	Grand father	Healthy carrier	Maternal	Unknown		19	Mat del	2537	0.8
							14	Pat WT	1561	94.7

Mat, maternal; pat, paternal; del, allele harbouring the IC1 deletion; WT, wild-type allele; CTS, CTCF target site.
Family has been previously described by: [a]Sparago *et al.* (10); [b]Prawitt *et al.* (12,19); [c]Cerrato *et al.* (13); [d]Sparago *et al.* (11); [e]De Crescenzo *et al.* (17).

there might be a kind of epigenetic memory effect, but an ascertainment bias cannot be excluded and more of these rare families must be investigated in more detail.

Control of *IGF2-H19* imprinting requires the enhancer-blocking activity of IC1 and this is exerted through interaction with CTCF (9,20,21,25). Consistent with the data on CTCF binding, we observed that the insulator activity of IC1 is modestly affected by the 2.2 kb (B5/B1) deletion but severely reduced by the 1.4 kb (B5/B3) and 1.8 kb (both B5/B2 and B6/B3) deletions. The comparable results obtained with the 1.8 kb (B5/B2) and 1.8 kb (B6/B3) deletions indicate that different CTSs play similar roles inside IC1. However, the dramatic differences between the 2.2 kb (B5/B1) and 1.4 kb (B5/B3) deletions indicate that the spatial arrangement of the CTSs rather than their overall number is important for the insulator function. We previously proposed that the deletions causing the formation of clusters of CTSs longer than those present in the WT allele (two clusters of three CTSs separated by 1 kb), such as the Δ 1.4 and Δ 1.8 kb (Fig. 1), would result in weak CTCF binding and enhancer-blocking activity (13). In contrast, deletions not changing the length of the CTS clusters, such as the Δ 2.2 kb, would have a milder effect. This model is corroborated and extended by the present study. Indeed, the *in vitro*-produced A2 deletion not removing any CTS but generating a long-CTS array severely affects the insulator activity and CTCF binding. In contrast, the serendipitously identified 0.8 kb (B3/B1) deletion removing two CTSs without increasing the length of the CTS clusters has a minor effect on these activities.

The A2 region contains OCT-binding sites, which have been found mutated in rare familial cases of BWS (15,20). The role of such sequences in the mouse *H19* ICR is controversial. A dyad OCT-binding sequence was implicated in the maintenance of the unmethylated state of the mouse *H19* ICR in a cell culture model (26). However, its deletion in the mouse has no effect on insulation and activation of the maternal *Igf2* allele (27). We found that mutating the three OCT-binding sites of the A2 region weakly affects the enhancer-blocking and CTCF-binding activities of IC1. Therefore, the effect of the A2 deletion on insulator activity and CTCF binding is in large part not due to the loss of the OCT-binding sites.

We observed that the efficiency of CTCF binding is influenced by the spatial arrangement of the target sites within human IC1. In particular, arrays of closely spaced CTSs longer than three appear to bind CTCF less efficiently. Interaction between adjacent CTSs has been demonstrated in the mouse (28). It is possible that steric interference occurs when CTCF molecules interact with multiple adjacent sites.

In summary, this study shows that depending on the structural arrangement of the remaining CTSs, microdeletions affect the insulator function of IC1 and clinical phenotype to a different extent. Severe inactivation, such as that observed with the 1.4–1.8 kb deletions, is associated with hypermethylation of the maternal IC1 allele *in vivo*. This condition is generally found in pedigrees showing highly penetrant BWS phenotype. In contrast, microdeletions causing moderate inactivation of IC1 function, such as the Δ 2.2 kb, are associated with stochastic DNA methylation of the maternal IC1 and incompletely penetrant clinical phenotype. According to the data obtained in cultured cells, we expect also the 0.8 kb deletion to

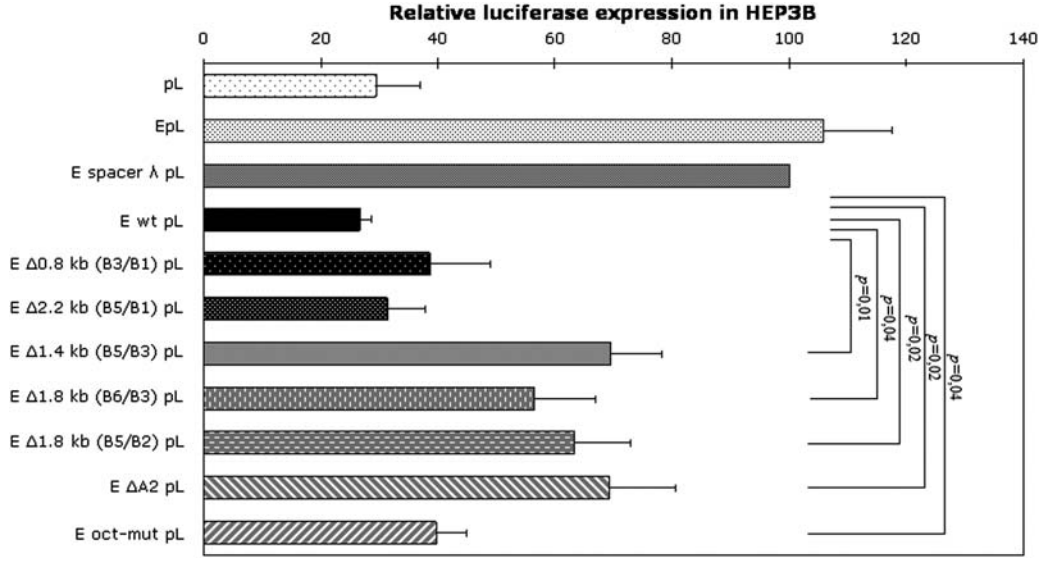

Figure 3. Enhancer-blocking assay. Hep3B cells were transfected with the constructs described in Figure 1. Pools of Neo^R-resistant clones were collected and their luciferase activity assayed. The activity expressed by the control construct containing the λ spacer was set as 100%. Data represent the average of three independent experiments and are expressed as the means ± SD. *P*-values calculated with Student's *t*-test are indicated, when statistically significant. Note that the Δ1.4 kb (B5/B3), Δ 1.8 kb (B6/B3), Δ 1.8 kb (B5/B2) and Δ A2 alleles display lower enhancer-blocking activity than the Δ 0.8 kb (B3/B1), Δ 2.2 kb (B5/B1), OCT-mut and WT alleles. EpL, plasmid without insert; pL, plasmid without enhancer and insert.

result in low-penetrance phenotype, if maternally transmitted. Careful genotyping of the IC1 microdeletions is therefore needed to predict recurrence risks and possible phenotypical outcomes. Furthermore, an in detail investigation of BWS cases with a *H19* hypermethylation regarding microdeletions should be considered even if no family history of BWS was observed.

MATERIALS AND METHODS

Materials

Genomic DNA was isolated from peripheral blood using the FlexiGene DNA Kit (Qiagen, Hilden, Germany) according to the manufacturer's manual. Blood samples were obtained after informed consent.

Methylation sensitive multiplex ligation-dependent probe amplification

Gene dosage and methylation of the IC1 and 2 on chromosome 11p15 were analysed by MLPA using the SALSA MLPA KIT ME030-B2 BWS/RSS (MRC Holland, Amsterdam, Netherlands). Hybridization, ligation and PCR reactions were carried out according to the manufacturer's instructions. Amplification products were analysed by capillary electrophoresis using the ABI3100 capillar sequencer. Data analysis was carried out using the Gene Marker Software (Softgenetics, State College, PA, USA).

Long-range PCR and sequencing

For confirmation of the deletion and identification of the breakpoints in individuals of family 8 long-range PCR was conducted using the Expand long-range dNTPack (Roche, Mannheim, Germany) according to the manufacturer's manual with primers H19_Del_F_longrange 5′-CCTCTATCT AATGACACGCTGTACTC-3′ and H19_Del_R_longrange 5′-GACTCAGGAAATACTCCGGAAATAC-3′. A 6.678 bp product was generated from a present WT -allele. PCR products were gel purified with the Gel extraction Kit (Qiagen, Hilden, Germany) according to the manufacturers' instructions. Sequencing of the breakpoints was performed with an additional primer (H19_nDNArev 5′-GGGCTGTCCTTA GACGGAGT-3′ (29) using the BigDye Terminator v1.1 Cycle Sequencing Kit on an ABI-3100 automatic capillary genetic analyser (Applied Biosystems, Fostercity, CA, USA). Sequence analysis was conducted using the Sequencing Analysis (Applied Biosystems, Fostercity, CA, USA) and Geneious (Biomatters, Auckland, New Zealand) softwares.

Bisulfite treatment

Bisulfite treatment was carried out as described elsewhere (30) or using the EZ DNA Methylation-Gold Kit (Zymo Research Europe, Freiberg, Germany) according to the manufacturer's protocol.

Generation of bisulfite amplicon libraries

Locus-specific amplicon libraries for each individual were generated. First, PCR on bisulfite treated DNA was performed with tagged primers using the Qiagen HotStarTaq Master Mix Kit (Qiagen, Hilden, Germany) and standard protocols. For primer sequences, see Supplementary Material, Table S4.

Sample-specific barcode sequences [(MIDs) multiplex identifiers] and universal linker tags (454 adaptor sequences, A- or B-primer and key) were added in a second PCR conducted as

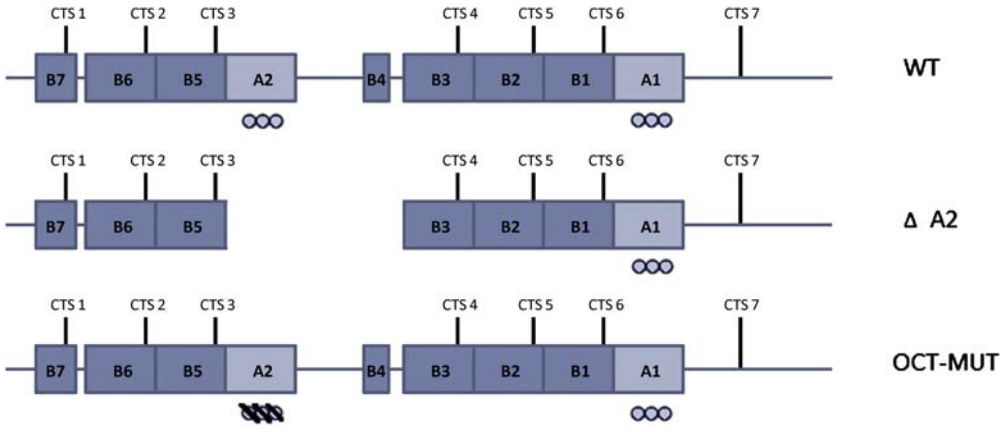

Figure 4. *In vitro*-generated IC1 mutations. Schematic diagram shows the *in vitro*-generated A2 deletion and OCT-mut alleles. The position of the OCT-binding motifs is indicated by small circles and the mutated OCT-binding motifs are slashed.

follows: 10 min denaturation at 95°C, then 35 cycles with 95°C for 20 s and 72°C for 30 s and a final elongation step for 7 min at 72°C.

Sample preparation and sequencing on the Roche/454 GS junior system

Amplicons were purified using the Agencourt AMPure XP Beads (Beckman Coulter, Krefeld, Germany) system according to the protocol recommended by Roche (Roche Amplicon Library Preparation Method Manual) and quantitated by measuring with the NanoDrop ND-1000 Spectrophotometer (ThermoScientific, Wilmington, USA). The bisulfite amplicon libraries were diluted, pooled and clonally amplified in an emulsion PCR (emPCR) and sequenced on the Roche/454 GS junior system according to the manufacturer's protocol (Roche emPCR Amplification Method Manual—Lib-A and Roche Sequencing Method Manual).

Data analysis

For data analyses, special filter settings were applied (for details contact KR). The obtained reads were sorted according to their MID by implementing an exact pattern-matching approach in the programming language Perl. The algorithm used identified whether either the forward or the reverse MID is present. If an MID was assigned to more than one amplicon, sequence reads for specific amplicon libraries were separated using the assembly tool of the Geneious Software (Biomatters, Auckland, New Zealand). Methylation analyses were conducted using the BiQAnalyzer HT (31). For each amplicon, a minimum number of 500 sequence reads was analysed. The mean methylation as a mean value for all CpGs studied, the exact number of reads analysed for the different samples and CTSs are given in Table 3 and Supplementary Material, Table S1. The average bisulfite conversion rate was 98.0% for all patients and 96.8% for the NCs.

Generation of the plasmid constructs

The plasmid constructs for the enhancer-blocking assay were generated as follows. The DNA sequence of the SV40 enhancer was PCR-amplified from plasmid pcDNA3.1 (Invitrogen) using primers 5′-TATATGGGGTACCGCGTTAC-3′ and 5′- GAGC TCGGGCGGAACTGG-3′. The obtained PCR product was digested with KpnI and SacI and subcloned between KpnI and XhoI sites in plasmid pGL3 (Promega) that is carrying a luciferase cassette under the control of the SV40 promoter. The resulting construct (EpL; Fig. 1B) was sequenced to verify the correct cloning. WT and mutant IC1 alleles were PCR-amplified from peripheral blood DNA with the primers:

5′- GTAGTGGCGCGCCATTTCCCAATG-3′ and 5′- GCA CAGGCGCGCCATCGA

ACATC-3′. The PCR products were digested with AscI and subcloned into the MluI site of the EpL vector. The correct cloning and orientation of the IC1 alleles were confirmed by DNA sequencing.

The EΔA2pL construct was obtained by deleting 1024 bp of the A2 region from the plasmid carrying WT IC1. The 513 bp *BsaAI-Bsu36I* fragment derived from WT IC1 was subcloned between *BmgBI* and *Bsu36I* sites in plasmid EwtpL. The correct mutagenesis was confirmed by sequencing.

The EOCT-mutpL construct was obtained by mutating the sequence of the A2 region containing the Octamer sites (underlined):

CATTAACATT CCCATTCAGT GCAGGTTTGA GATG CTAATT TAGGAGCTTG AGATGCTAAA into: CA**GG** A**TTT**TT CCCATTCAGT GCAGGTTTGA GA**AAA**T **CC**TT TAGGAGCTTG AGA**AAATCC**A (mutated nucleotides are in bold). This has been achieved subcloning sequentially the following synthetic DNA fragments: 5′-CTT AAGTGGCCAGACAGGATTTTTCCCATTCAGTGCAGG TTTGAGAAAATCCTTTAGGAGCTTGAGAAAATCCAGA GCTGGGAGTGCCACTGCTGCTTTATTCTGGGGTCTAG GATCC-3′ and 5′-GGATCCTTGTGTTGGCTGAGATAATC TGCTAAT

GTGGGTGCAGCAGACATCCCGCGGTTTGTGGAATC GATAAGCTT-3′ in AflII-BamHI and BamHI-HindIII,

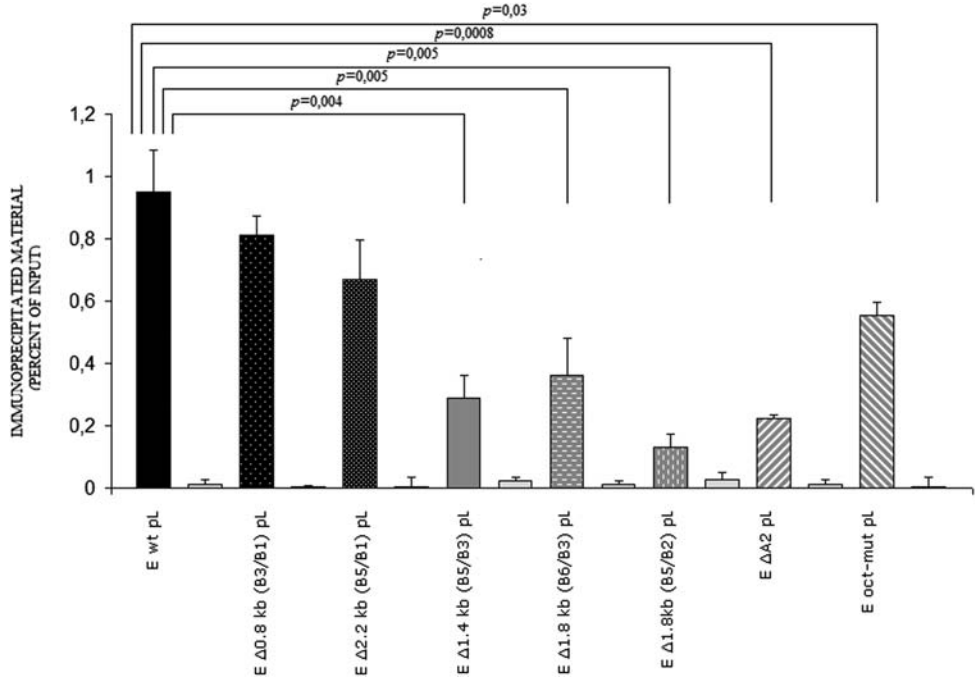

Figure 5. Chromatin ImmunoPrecipitation assay. Chromatin extracted from Hep3B cells transfected with the constructs described in Supplementary Material, Fig. S2 was immunoprecipitated with anti-CTCF antibodies. The amount of exogenous IC1 DNA present in the immunoprecipitated material was estimated by real-time PCR and expressed as percent of input. IC1 values were normalized against the values obtained for an endogenous high-affinity CTCF-binding region. Data represent the average of three independent experiments and are expressed as the means ± SD. *P*-values calculated with Student's *t*-test are indicated, when statistically significant. The results shown have been obtained by using primers specific for the CTS1 region. Similar results have been obtained by using primers for a region close to CTS6 (Supplementary Material, Fig. S4). Primers for an endogenous region with no known CTCF binding were used to measure non-specific binding (grey bars). Note that the efficiency of CTCF binding to the Δ 1.4 kb (B5/B3), Δ 1.8 kb (B6/B3), Δ 1.8 kb (B5/B2) and Δ A2 IC1 alleles is lower than that to the Δ 0.8 kb (B3/B1), Δ 2.2 kb (B5/B1), OCT-mut and WT alleles.

respectively, of topo TA vector (Promega). The resulting AflII-ClaI fragment has then been inserted between AflII and ClaI sites of the WT IC1 sequence.

Cell culture and transfections

Hep3b cells were cultured in Dulbecco's modified Eagle's medium (Sigma Co. Ltd, St Louis, MO, USA) supplemented with 10% fetal bovine serum, 50 units of penicillin and 50 μg/ml of streptomycin at 37°C under an atmosphere of 5% CO_2. For the evaluation of enhancer-blocking activity, Hep3b were transfected in triplicate.

Cells were seeded in six-well plates (Nunc Co., Roskilde, Denmark) at a density of 1×10^5 cells per well. The day after cell seeding, 4 μg of SalI-linearized plasmid and 0.4 μg of SalI-linearized PGK-neo vector were mixed with Lipofect Amine Plus reagent and the mixture was added to each dish. The cells were trypsinized and seeded on to 100 mm plates (Nunc Co). 48 h later, 200 μg/ml of neomycin (Sigma Co. Ltd) were added to the medium for at least 5 days in order to select the stably transfected clones. All neomycin-resistant clones were pooled and analyzed.

Luciferase assay for enhancer-blocking activity

The luciferase activity was measured using the Luciferase Assay System (Promega Co.) and Dia-Iatron luminometer, following the protocols described by the manufacturer. Firefly luciferase activity was normalized against protein concentration and plasmid copy number, and the relative luciferase activities were expressed as the percentage of the construct containing the λ spacer. Protein concentrations were determined by the Bradford method (Bio-Rad, Hercules, CA, USA).

Chromatin ImmunoPrecipitation

Hep3b cells were fixed with 1% formaldehyde for 15 min at room temperature. The cells were lysed, and the chromatin was sonicated to an average size of 600 bp. For each experiment, 100 μg of chromatin were immunoprecipitated with 4 μg of anti-CTCF or anti H3 antibodies (by Upstate and Abcam, respectively) according to the manufacturer's protocols. The amount of IC1-containing DNA fragments present in the immunoprecipitated material was estimated by quantitative PCR. The samples were normalized against an endogenous region (23). For the analysis of CTS1, amplicons spanning the plasmid-insert boundaries were generated. Primers for CTS1 were:

5′-AGCAACCAGGTGTGGAAAGT-3′ and 5′-ATGCATG GGCTCCTAGACAG-3′.

Primers for analysing CTS6 were: 5′-TCTTCAGGTCGG GCATTATC-3′ and 5′- TTAGACGGAGTCGGAGCTGT-3′. Primers for the CTCF binding control region at chromosome 6 were: 5′-CAGCTCTGTGTCCTGTCTTATCC-3′ and 5′-CAGCTATAATTGATGAAGAGGCG-3′ (23). Primers for a

distant element with no known CTCF binding (chromosome 5) were: 5′-GCTGTGCTGAGAGTGAGGC-3′ and 5′-GGCT GAGCACTAAGATGCTG-3′ (23).

SUPPLEMENTARY MATERIAL

Supplementary Material is available at *HMG* online.

ACKNOWLEDGEMENT

We thank the patients and families for their cooperation and the physicians for patient referrals, Deniz Kanber, Beate Albrecht and Frank Dechend for helpful discussions, Nicholas Wagner for helpful support on the Roche/454 Genome Sequencing junior system and Stephanie Groß for expert technical assistance.

Conflict of Interest statement. None declared.

FUNDING

This work was supported by grants from MIUR PRIN 2007 and PRIN 2009 (to A.R. and M.V.C.), Telethon-Italia grant no. GGP11122 and Progetto Bandiera MIUR-CNR Epigenomica (to A.R.), Associazione Italiana Ricerca sul Cancro (to A.R. and F.C.) and the Bundesministerium für Bildung und Forschung (Network Imprinting diseases, 01GM1114A to B.H. and K.B., and 01GM1114D to D.P.). Funding to pay the Open Access Publication charges for this article was provided by Fondazione Telethon-Italia.

REFERENCES

1. Choufani, S., Shuman, C. and Weksberg, R. (2010) Beckwith-Wiedemann syndrome. *Am. J. Med. Genet. C. Semin. Med. Genet.*, **154C**, 343–354.
2. Cerrato, F., Sparago, A., Di Matteo, I., Zou, X., Dean, W., Sasaki, H., Smith, P., Genesio, R., Bruggemann, M., Reik, W. and Riccio, A. (2005a) The two-domain hypothesis in Beckwith–Wiedemann syndrome: autonomous imprinting of the telomeric domain of the distal chromosome 7 cluster. *Hum. Mol. Genet.*, **14**, 503–511.
3. Bartolomei, M.S. (2009) Genomic imprinting: employing and avoiding epigenetic processes. *Genes Dev.*, **23**, 2124–2133.
4. Ferguson-Smith, A.C. (2011) Genomic imprinting: the emergence of an epigenetic paradigm. *Nat. Rev. Genet.*, **12**, 565–575.
5. Bartolomei, M.S. and Ferguson-Smith, A.C. (2011) Mammalian genomic imprinting. *Cold Spring Harb. Perspect. Biol.*, **3**. doi: 10.1101/cshperspect.a002592.
6. Nativio, R., Sparago, A., Ito, Y., Weksberg, R., Riccio, A. and Murrell, A. (2011) Disruption of genomic neighbourhood at the imprinted *IGF2-H19* locus in Beckwith–Wiedemann syndrome and Silver-Russell syndrome. *Hum. Mol. Genet.*, **20**, 1363–1374.
7. Murrell, A., Heeson, S. and Reik, W. (2004) Interaction between differentially methylated regions partitions the imprinted genes Igf2 and H19 into parent-specific chromatin loops. *Nat. Genet.*, **36**, 889–893.
8. Kurukuti, S., Tiwari, V.K., Tavoosidana, G., Pugacheva, E., Murrell, A., Zhao, Z., Lobanenkov, V., Reik, W. and Ohlsson, R. (2006) CTCF binding at the H19 imprinting control region mediates maternally inherited higher-order chromatin conformation to restrict enhancer access to Igf2. *Proc. Natl Acad. Sci. U S A*, **103**, 10684–10689.
9. Schoenherr, C.J., Levorse, J.M. and Tilghman, S.M. (2003) CTCF maintains differential methylation at the Igf2/H19 locus. *Nat. Genet.*, **33**, 66–69.
10. Sparago, A., Cerrato, F., Vernucci, M., Ferrero, G.B., Cirillo Silengo, M. and Riccio, A. (2004) Microdeletions in the human H19 DMR result in loss of IGF2 imprinting and Beckwith–Wiedemann. *Nat. Genet.*, **36**, 958–960.
11. Sparago, A., Russo, S., Cerrato, F., Ferraiuolo, S., Castorina, P., Selicorni, A., Schwienbacher, C., Negrini, M., Ferrero, G.B., Silengo, M.C. *et al.* (2007) Mechanisms causing imprinting defects in familial Beckwith–Wiedemann syndrome with Wilms' tumour. *Hum. Mol. Genet.*, **16**, 254–264.
12. Prawitt, D., Enklaar, T., Gartner-Rupprecht, B., Spangenberg, C., Oswald, M., Lausch, E., Schmidtke, P., Reutzel, D., Fees, S., Lucito, R. *et al.* (2005a) Microdeletion of target sites for insulator protein CTCF in a chromosome 11p15 imprinting center in Beckwith–Wiedemann syndrome and Wilms' tumour. *Proc. Natl Acad. Sci. U S A*, **102**, 4085–4090.
13. Cerrato, F., Sparago, A., Farina, L., Ferrero, G.B., Cirillo Silengo, M. and Riccio, A. (2005b) Microdeletion and IGF2 loss of imprinting in a cascade causing Beckwith-Wiedemann syndrome with Wilms' tumor—reply. *Nat. Genet.*, **37**, 786–787.
14. Cerrato, F., Sparago, A., Verde, G., De Crescenzo, A., Citro, V., Cubellis, M.V., Rinaldi, M.M., Boccuto, L., Neri, G., Magnani, C. *et al.* (2008) Different mechanisms cause imprinting defects at the IGF2/H19 locus in Beckwith-Wiedemann syndrome and Wilms' tumour. *Hum. Mol. Genet.*, **17**, 1427–1435.
15. Demars, J., Ennuri Shmela, M., Rossignol, S., Okabe, J., Netchine, I., Azzi, S., Cabrol, S., Le Caignec, C., David, A., Le Bouc, Y., El-Osta, A. and Cicquel, C. (2010) Analysis of the IFG2/H19 imprinting control region uncovers new genetic defects, including mutations of OCT-binding sequences in patients with 11p15 fetal growth disorders. *Hum. Mol. Genet.*, **19**, 803–814.
16. Demars, J., Rossignol, S., Netchine, I., Lee, K.S., Shmela, M., Faivre, L., Weill, J., Odent, S., Azzi, S., Callier, P. *et al.* (2011) New insights into the pathogenesis of Beckwith-Wiedemann and Silver-Russell syndromes: contribution of small copy number variations to 11p15 imprinting defects. *Hum. Mutat.*, **32**, 1171–1182.
17. De Crescenzo, A., Coppola, F., Falco, P., Bernardo, I., Ausanio, G., Cerrato, F., Falco, L. and Riccio, A. (2011) A novel microdeletion in the IGF2/H19 imprinting centre region defines a recurrent mutation mechanism in familial Beckwith-Wiedemann syndrome. *Eur. J. Med. Genet.*, **54**, e451–e454.
18. Scott, R.H., Douglas, J., Baskcomb, L., Huxter, N., Barker, K., Hanks, S., Craft, A., Gerrard, M., Kohler, J.A., Levitt, G.A., Picton, S., Pizer, B., Ronghe, M.D., Williams, D., Cook, J.A., Pujol, P., Maher, E.R., Birch, J.M., Stiller, C.A., Pritchard-Jones, K. and Rahman, N. (2008) Factors Associated with Childhood Tumours (FACT) Collaboration Constitutional 11p15 abnormalities, including heritable imprinting center mutations, cause nonsyndromic Wilms tumor. *Nat. Genet.*, **40**, 1329–1334.
19. Prawitt, D., Enklaar, T., Gärtner-Rupprecht, B., Spangenberg, C., Lausch, E., Reutzel, D., Fees, S., Korzon, M., Brozek, I., Limon, J., Housman, D.E., Pelletier, J. and Zabel, B. (2005b) Microdeletion and IGF2 loss of imprinting in a cascade causing Beckwith-Wiedemann syndrome with Wilms' tumor. *Nat. Genet.*, **37**, 785–786.
20. Poole, R.L., Leith, D.J., Docherty, L.E., Shmela, M.E., Gicquel, C., Splitt, M., Temple, I.K. and Mackay, D.J. (2012) Beckwith-Wiedemann syndrome caused by maternally inherited mutation of an OCT-binding motif in the IGF2/H19-imprinting control region, ICR1. *Eur. J. Hum. Genet.*, **20**, 240–243.
21. Hark, A.T., Schoenherr, C.J., Katz, D.J., Ingram, R.S., Levorse, J.M. and Tilghman, S.M. (2000) CTCF mediates methylation-sensitive enhancer-blocking activity at the H19/Igf2 locus. *Nature*, **405**, 486–489.
22. Bell, A.C. and Felsenfeld, G. (2000) Methylation of a CTCF-dependent boundary controls imprinted expression of the Igf2 gene. *Nature*, **405**, 482–485.
23. Wendt, K.S., Yoshida, K., Itoh, T., Bando, M., Koch, B., Schirghuber, E., Tsutsumi, S., Nagae, G., Ishihara, K., Mishiro, T. *et al.* (2008) Cohesin mediates transcriptional insulation by CCCTC-binding factor. *Nature*, **451**, 796–801.
24. Szabó, P.E., Tang, S.H., Silva, F.J., Tsark, W.M. and Mann, J.R. (2004) Role of CTCF binding sites in the Igf2/H19 imprinting control region. *Mol. Cell. Biol.*, **24**, 4791–4800.
25. Pant, V., Mariano, P., Kanduri, C., Mattsson, A., Lobanenkov, V.V., Heuchel, R. and Ohlsson, R. (2003) The nucleotides responsible for the direct physical contact between the chromatin insulator protein CTCF and the H19 imprinting control region manifest parent of origin-specific long-distance insulation and methylation-free domains. *Genes Dev.*, **17**, 586–590.
26. Hori, N., Nakano, H., Takeuchi, T., Kato, H., Hamaguchi, S., Oshimura, M. and Sato, K. (2002) A dyad OCT-binding sequence functions as a

maintenance sequence for the unmethylated state within the *H19/Igf2*-imprinted control region. *J. Biol. Chem.*, **277**, 27960–27967.
27. Ideraabdullah, F.Y., Abramowitz, L.K., Thorvaldsen, J.L., Krapp, C., Wen, S.C., Engel, N. and Bartolomei, M.S. (2011) Novel cis-regulatory function in ICR-mediated imprinted repression of H19. *Dev. Biol.*, **355**, 349–57.
28. Pant, V., Kurukuti, S., Pugacheva, E., Shamsuddin, S., Mariano, P., Renkawitz, R., Klenova, E., Lobanenkov, V. and Ohlsson, R. (2004) Mutation of a single CTCF target site within the H19 imprinting control region leads to loss of Igf2 imprinting and complex patterns of de novo methylation upon maternal inheritance. *Mol. Cell. Biol.*, **24**, 3497–3504.
29. Zeschnigk, M., Albrecht, B., Buiting, K., Kanber, D., Eggermann, T., Binder, G., Gromoll, J., Prott, E.C., Seland, S. and Horsthemke, B. (2008) IGF2/H19 hypomethylation in Silver-Russell syndrome and isolated hemihypoplasia. *Eur. J. Hum. Genet.*, **16**, 328–334.
30. Kanber, D., Buiting, K., Zeschnigk, M., Ludwig, M. and Horsthemke, B. (2009) Low frequency of imprinting defects in ICSI children born small for gestational age. *Eur. J. Hum. Genet.*, **17**, 22–29.
31. Lutsik, P., Feuerbach, L., Arand, J., Lengauer, T., Walter, J. and Bock, C. (2011) BiQ Analyzer HT: locus-specific analysis of DNA methylation by high-throughput bisulfite sequencing. *Nucleic Acids Res.*, **39**, (Web Server issue), W551–W556.